# The brain-specific double-stranded RNA-binding protein Staufen2 is required for dendritic spine morphogenesis

Bernhard Goetze,[1,2] Fabian Tuebing,[1,2] Yunli Xie,[1,2] Mario M. Dorostkar,[3] Sabine Thomas,[1,2] Ulrich Pehl,[4] Stefan Boehm,[3] Paolo Macchi,[1,2] and Michael A. Kiebler[1,2]

[1]Max-Planck-Institute for Developmental Biology, 72076 Tübingen, Germany
[2]Center for Brain Research and [3]Institute for Pharmacology, Medical University of Vienna, A-1090 Vienna, Austria
[4]Department of Drug Discovery Support, General Pharmacology Group, Boehringer Ingelheim Pharma GmbH & Co. KG, 88397 Biberach, Germany

Mammalian Staufen2 (Stau2) is a member of the double-stranded RNA-binding protein family. Its expression is largely restricted to the brain. It is thought to play a role in the delivery of RNA to dendrites of polarized neurons. To investigate the function of Stau2 in mature neurons, we interfered with Stau2 expression by RNA interference (RNAi). Mature neurons lacking Stau2 displayed a significant reduction in the number of dendritic spines and an increase in filopodia-like structures. The number of PSD95-positive synapses and miniature excitatory postsynaptic currents were markedly reduced in Stau2 down-regulated neurons. Akin effects were caused by overexpression of dominant-negative Stau2. The observed phenotype could be rescued by overexpression of two RNAi cleavage-resistant Stau2 isoforms. In situ hybridization revealed reduced expression levels of β-*actin* mRNA and fewer dendritic β-*actin* mRNPs in Stau2 down-regulated neurons. Thus, our data suggest an important role for Stau2 in the formation and maintenance of dendritic spines of hippocampal neurons.

## Introduction

Local translation of certain mRNAs at synapses in response to activation critically contributes to asymmetric cell polarity and synaptic plasticity (Kiebler and DesGroseillers, 2000; Steward and Schuman, 2001; St Johnston, 2005). The double-stranded RNA-binding protein Staufen has been implicated both in dendritic RNA transport and translational regulation (Tang et al., 2001; Kim et al., 2005). In *Drosophila*, Staufen (Stau) is required for both *bicoid* and *oskar* mRNA localization in the oocyte (St Johnston, 2005) and for the localization of *prospero* mRNA in embryonic neuroblasts (Li et al., 1997; Broadus et al., 1998). In *Xenopus*, two Staufen isoforms (XStau1 and XStau2) are present in the oocytes and move to the vegetal cytoplasm, where both *VegT* and *Vg1* mRNAs become localized (Allison et al., 2004; Yoon and Mowry, 2004). In mammals, Stau1 and 2 proteins are implicated in the microtubule-dependent transport of RNAs to dendrites of polarized neurons (Kiebler et al., 1999; Tang et al., 2001). Both Stau proteins are present in ribonucleoprotein particles (RNPs) in the cell body and dendrites (Kiebler et al., 1999; Duchaîne et al., 2002; Kanai et al., 2004; Thomas et al., 2005). Due to alternative splicing, four Stau2 isoforms are expressed in rat brain with molecular weights ranging from 52 to 62 kD (Duchaîne et al., 2002; Monshausen et al., 2004). A first indication that Staufen proteins may actually contact their cargo RNAs already inside the nucleus came from recent work demonstrating that two isoforms of Stau2, Stau2$^{62}$ and Stau2$^{59}$, are imported into the nucleus and then become exported via exportin-5 (Brownawell and Macara, 2002; Macchi et al., 2004; Kiebler et al., 2005) and exportin-1 (CRM1; Miki and Yoneda, 2004), respectively. The function of the brain-specific Stau2 in the central nervous system is, however, still elusive. Therefore, we investigated the function of Stau2 by RNA interference (RNAi) in polarized hippocampal neurons.

## Results

To determine at which stage of neuronal development Stau2 is expressed, we performed semi-quantitative RT-PCR on RNA extracted from cultured hippocampal neurons at different days in vitro (DIV) (see Fig. S1 A, available at http://www.jcb.org/cgi/content/full/jcb.200509035/DC1). Stau2 mRNA could be

Correspondence to: paolo.macchi@meduniwien.ac.at

Abbreviations used in this paper: DIV, days in vitro; FMRP, Fragile X mental retardation protein; mEPSC, miniature excitatory postsynaptic current; RNAi, RNA interference; shRNA, short hairpin RNA; siRNA, small interfering RNA; TLS, translocated in liposarcoma.

The online version of this article contains supplemental material.


The Journal of Cell Biology, Vol. 172, No. 2, January 16, 2006 221–231
http://www.jcb.org/cgi/doi/10.1083/jcb.200509035

detected at all stages examined, indicating that Stau2 is expressed throughout neuronal development. We then performed loss-of-function analyses using RNAi in polarized hippocampal neurons to investigate the function of Stau2. Two 19mer oligonucleotides directed against different regions of the Stau2 cDNA were cloned into the pSUPER vector (Brummelkamp et al., 2002). Their expression yields short hairpin RNAs (shRNAs) that are subsequently converted into small interfering RNAs (siRNAs). Cotransfection of HeLa cells with either of the two plasmids, si2-1 (unpublished data) or si2-2 (Fig. S1 B), together with Stau2-EYFP significantly down-regulated Stau2-EYFP expression as assessed by fluorescence microscopy. In contrast, neither of these plasmids affected the level of the paralogous protein, Stau1-EYFP (Fig. S1 B). Furthermore, a control Stau2 siRNA with 5 bp substitutions (mismatch siRNA) did not affect the level of Stau2-EYFP expression (unpublished data).

We then determined the level and the specificity of Stau2 down-regulation in neurons by Western blot analyses. Primary hippocampal neurons were transfected by nucleoporation (Hamm et al., 2002) before plating with plasmids yielding shRNAs against Stau2 (si2-2) and an unrelated protein, CDC10 (siCDC10, negative control). As additional controls, neurons were either mock treated (citrine) or transfected with pSUPER vector expressing the mismatch sequence of si2-2 (mis) (Fig. 1 A). Neurons were allowed to develop for 3 d and processed for Western blot analysis. Only siRNAs directed against Stau2 significantly down-regulated the expression of three Stau2 isoforms (62, 59, and 52 kD), whereas all other control plasmids did not (Fig. 1 A). The same results were obtained by using short interfering oligos (Dharmacon) (Fig. S1 C). Importantly, we did not observe any compensatory change in Stau1 expression levels upon Stau2 down-regulation (Fig. 1 A, bottom). To verify down-regulation of Stau2 in mature cells, 15 DIV neurons were cotransfected with plasmids encoding cyan fluorescent protein (ECFP) and si2-2 RNA, and immunostaining was performed for Stau2 3 d after transfection. Both Stau2 shRNAs, si2-2 and si2-1, reduced or completely abolished Stau2 expression in neurons (Fig. 1 B, and unpublished data). Stau2 signal in dendrites was strongly reduced in Stau2 down-regulated neurons compared with untransfected cells (Fig. 1 B, enlarged insets). Neither mismatch shRNA against Stau2 (Fig. 1 B) nor shRNA against red fluorescent protein (RFP) (unpublished data) affected Stau2 expression. Moreover, the expression level of Stau1 remained unchanged (Fig. 1 B, middle), suggesting that this RNAi approach targeting Stau2 was specific.

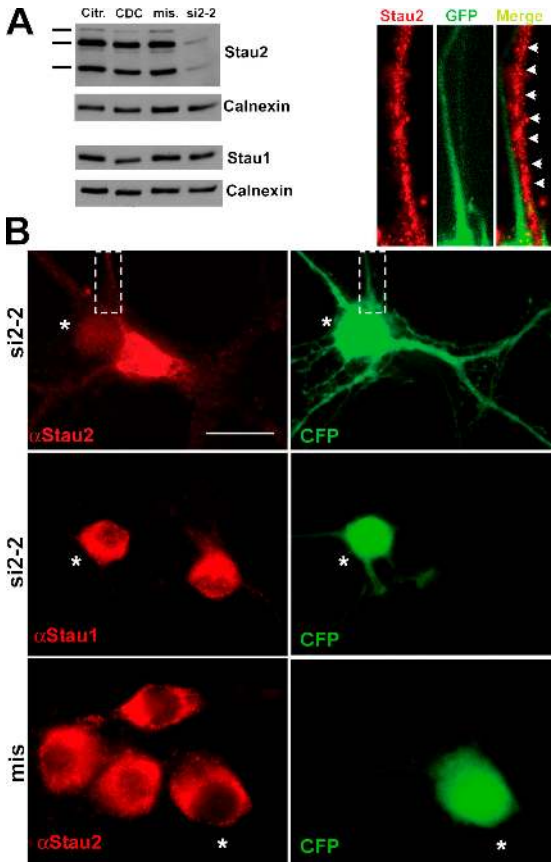


Figure 1. **Sequence-specific silencing of Staufen 2 by RNAi.** (A) Western blot analysis of transfected hippocampal neurons. Neurons were cotransfected with a plasmid expressing citrine fluorescent protein (lane 1, Citr.) and shRNA-expressing plasmids against CDC10 (lane 2, CDC), mismatch Stau2 (lane 3, mis), and Stau2 (lane 4, si2-2). Cells were lysed after 3 d of expression and processed for Western blotting. Levels of the three Stau2 isoforms (lines denote 62, 59, and 52 kD, respectively) were significantly down-regulated in cells transfected with si2-2 (lane 4). Calnexin served as internal loading control. Levels of Stau1 remained constant as revealed by decoration with anti-Stau1 antibodies (bottom). (B) Down-regulation of Stau2 in neurons. 15 DIV neurons were cotransfected with pSUPER vector (si2-2 or mismatch) together with ECFP (green). Neurons were stained 3 d after transfection with anti-Stau2 or anti-Stau1 antibodies (red). Stau2 signal was strongly reduced in both the cell body (asterisk) and dendrites (enlarged insets) of transfected neurons (green) compared with untransfected neurons (arrowheads in inset). However, as RNAi does not completely eliminate Stau2, a residual Stau2 staining was often still detected in dendrites. In contrast, expression of misStau2 or si-RFP (not depicted) did not alter the Stau2 level. Down-regulation of Stau2 also did not affect Stau1 expression level. Asterisk indicates the position of CFP-expressing neurons. Bar, 10 μm.

## Stau2 down-regulation in mature neurons decreases the number of dendritic spines

We first assessed the subcellular localization of Stau2 in dendrites of mature hippocampal neurons (Fig. 2) and asked whether Stau2 is present near synapses. Immunostaining using affinity-purified anti-Stau2 antibodies and mAbs specific for the postsynaptic marker protein PSD95 revealed that discrete Stau2 particles were distributed along the dendritic shaft beneath PSD95-positive puncta. The distribution of such Stau2 RNPs was not homogenous, but in close proximity to dendritic spines (Fig. 2). This was a first indication that Stau2 might actually play a role in synapse formation or maintenance of dendritic spines.

This prompted us to analyze whether down-regulation of Stau2 expression by RNAi in 15 DIV neurons alters dendritic spine morphology. Neurons expressing EYFP showed normal mushroom-like dendritic spines (Fig. 3 A, EYFP; see arrowheads). In contrast, expression of both si2-1 and si2-2 shRNAs resulted in an altered phenotype: the number of protrusions was significantly reduced, whereas extended filopodia appeared (Fig. 3 A, see arrows and inset). Both structures can be discriminated based on their morphology because dendritic

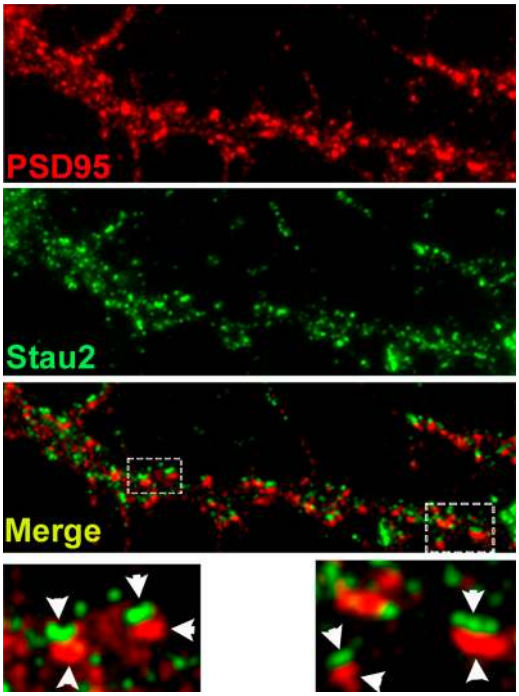


Figure 2. **Dendritic localization of endogenous Stau2.** Immunostaining for PSD95 (red) and Stau2 (green) performed in 15 DIV neurons. The two insets show a high magnification of the merged picture. Arrowheads indicate adjacent PSD95 puncta and Stau2 particles.

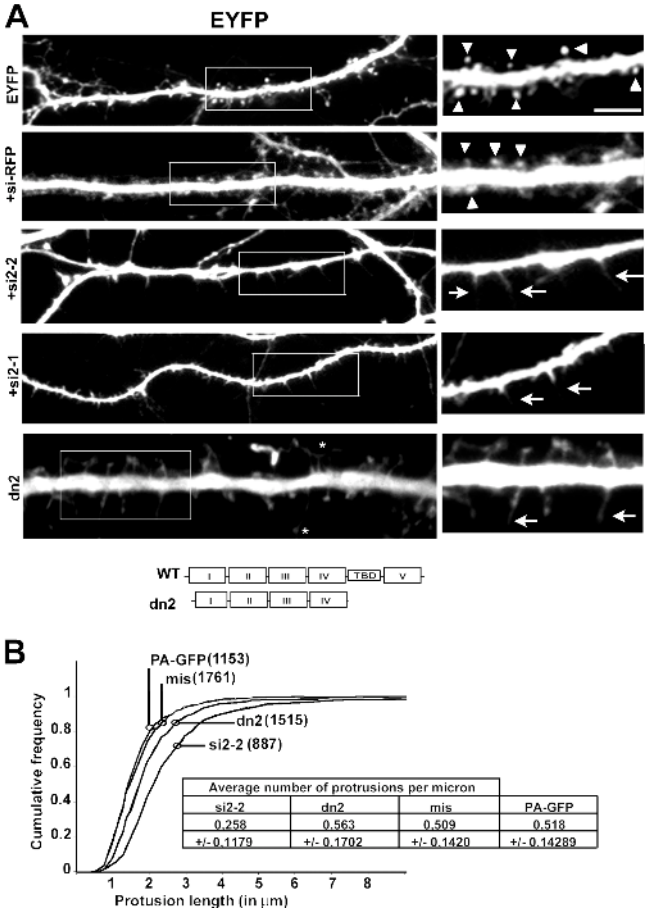


Figure 3. **Down-regulation of Stau2 reduces the number of dendritic spines.** (A) Representative images of the observed phenotype. 15 DIV neurons were transfected with a transfection marker (photo-activatable [PA] GFP or citrine) together with si2-1, si-2-2, si-RFP shRNAs, or with a plasmid expressing a dominant-negative Stau2 (dn2). After 3 d of expression, neurons were fixed and analyzed. Panels on the right are enlargements of the boxed areas (dendrites). Both Stau2 shRNAs cause a decrease in the number of dendritic spines even though the effect of si2-2 was more penetrant. Arrowheads indicate dendritic spines, arrows indicate extended filopodia. Schematic representation of wild-type Stau2 and dn2 proteins (bottom). The RNA binding domains are numbered; TBD, tubulin binding domain. (B) Quantification of the cells shown in A. Staufen2 down-regulation increased the length of protrusions as shown in cumulative frequency distributions. Two independent experiments have been performed and 5,316 protrusions were counted from 148 dendrites derived from 37 neurons. The total number of counted protrusions per condition is indicated in parentheses. The average number of protrusions per µm dendrite length for each condition is indicated in the inset. Bar, 1 µm.

spines are usually less than 2 µm, filopodia in contrast are usually longer (Hering and Sheng, 2001).

Although RNAi is thought to display a high degree of specificity and to act on selective targets, it may activate the Jak–Stat pathway, yielding retrograde dendritic retraction and inhibiting synapse formation in neurons (Kim et al., 2002; Sledz et al., 2003). We, therefore, devised control experiments to determine whether the observed phenotype was specific for Stau2. First, expression of an unrelated shRNA directed against RFP did not affect the morphology of dendritic spines (Fig. 3 A, siRFP). Second, a Stau2 shRNA that contains mismatches does not alter the morphology of dendritic spines (unpublished data and Fig. 3 B). Third, we expressed a truncated form of Stau2 (dn2) missing its COOH terminus, which has been shown to accumulate in the cell body, thereby acting as a dominant-negative protein (Tang et al., 2001). Interestingly, this frequently caused a change in morphology of dendritic spines displaying an extended neck (Fig. 3 A, see asterisk). Overexpression of dn2, therefore, yields an intermediate phenotype compared with wild-type and si-2–treated neurons (see Fig. 3 B). It is important to note that overexpression of full-length Stau2 does not yield the same phenotype (see also Fig. 6). Collectively, these controls demonstrate that our RNAi approach against Stau2 is indeed specific.

To quantify the observed effects, the length of protrusions was measured and the percentage of protrusions longer than 2 µm was determined. We observed a 10-fold increase in the percentage of extended protrusions in Stau2 down-regulated neurons, compared with siRFP or EYFP-transfected neurons (Fig. S1 D). Fig. 3 B shows a cumulative frequency plot of the measured protrusion lengths underlining the increase in long protrusions upon Stau2 down-regulation or overexpression of dn2. In total, Stau2 down-regulation causes a 49.4% loss of protrusions compared with mismatch shRNA (Fig. 3 B, inset). Collectively, down-regulation of Stau2 critically alters the morphology of protrusions from dendritic spines toward extended filopodia as well as their total number.

### Stau2 down-regulation in mature neurons decreases the number of synapses

A criterion for mature excitatory synapses is the presence of postsynaptic densities (PSDs) that cluster neurotransmitter receptors, in close contact with presynaptic nerve terminals.

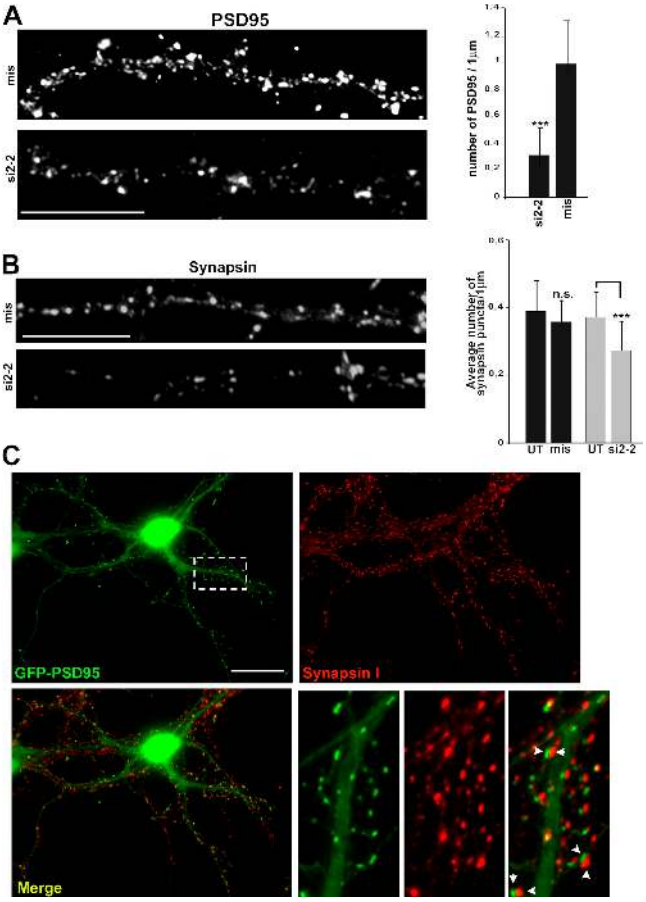


Figure 4. **Stau2 down-regulation reduces both the number of endogenous PSD95 and synapsinI puncta.** (A) Endogenous PSD95 immunostainings. 15 DIV neurons expressing the pSUPERIOR misStau2 or si2-2 vectors were immunostained for the postsynaptic marker PSD95. A reduction of 68% was observed in Stau2 down-regulated neurons compared with mismatch. In total, 25 and 29 dendrites were analyzed for si-2 and mis-treated neurons, respectively, and a total of 690 and 2,226 PSD95 puncta were counted. (B) Endogenous synapsinI immunostainings. 15 DIV neurons expressing the pSUPERIOR misStau2 or si2-2 vectors were immunostained for the presynaptic marker synapsinI. A reduction of 26% (***, $P < 0.0001$) in synapsinI puncta was observed in Stau2 down-regulated neurons compared with mismatch. In total, 36 and 39 dendrites of 6 neurons were analyzed for si-2 and mis-treated neurons, respectively, and a total of 273 and 464 synapsinI puncta were counted. (C) Most GFP-PSD95 clusters adjoin synapsinI. 15 DIV neurons were transfected with GFP-PSD95, fixed and immunostained for synapsinI 3 d later. Insets show enlargements of a dendritic segment where most postsynaptic dendritic spines (green) receive presynaptic input (red). Arrowheads indicate adjacent GFP-PSD95 and synapsinI puncta. Bars, 10 µm.

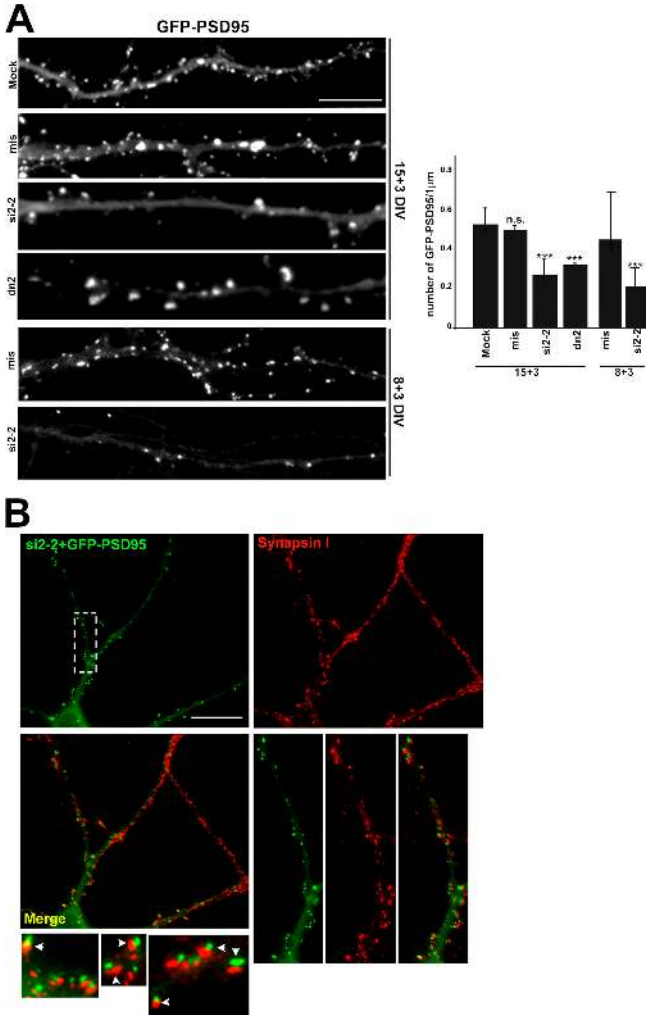


Figure 5. **Stau2 down-regulation reduces the number of GFP-PSD95 puncta.** (A) Overexpression of GFP-PSD95 in Stau2 down-regulated and control neurons. 15 DIV and 8 DIV hippocampal neurons were cotransfected with GFP-PSD95 and one of the following plasmids: empty vector (mock), mis, si2-2, or dn2. Cells were fixed 3 d after transfection. The number of GFP-PSD95 puncta that were found outside of the dendritic shaft was determined per µm dendrite length. For Stau2 down-regulated neurons, the number of GFP-PSD95 puncta was reduced by 48% ± 14.8% (***, $P < 0.0001$). Overexpression of ds2 had a similar effect (39% ± 0.8% reduction; ***, $P < 0.0001$). For 15 DIV neurons, 95 cells were analyzed and 9,203 dendritic spines were counted; for 8 DIV neurons, 53 cells were analyzed and 4,683 dendritic spines were counted. The graph represents a representative example of three independent experiments. Error bars represent the SD; n.s., statistically not significant. (B) SynapsinI immunostaining in GFP-PSD95 transfected neurons lacking Stau2. A significant reduction in GFP-PSD95 clusters was observed in Stau2 down-regulated neurons (see Fig. 4 and quantification therein). The majority of the remaining GFP-PSD95–positive dendritic spines still receive presynaptic input as shown in the enlarged dendritic segment and in the higher magnifications below. Arrowheads indicate adjacent GFP-PSD95 and synapsinI puncta. Bar, 10 µm.

We first determined whether Stau2 down-regulation affected the number of endogenous PSD95. Hippocampal neurons were stained with an anti-PSD95 antibody upon expression of either mismatched (control) or si2-2 pSUPERIOR plasmid. PSD95-positive puncta were quantified as described previously (Goetze et al., 2004). As expected, the number of PSD95 clusters per 1 µm dendrite length was reduced significantly, by 68% in Stau2 down-regulated neurons compared with mismatch shRNA-treated neurons (si2-2: 0.99 ± 0.33, mis: 0.31 ± 0.21) (Fig. 4 A). In contrast, the number of PSD95 puncta in mismatch shRNA-treated neurons was not altered compared with untransfected neurons (unpublished data).

We next asked the question of whether the presynaptic input was also affected by the Stau2 shRNA approach. Neurons were stained with a polyclonal anti-synapsinI antibody upon expression of either mismatch (control) or si2-2 pSUPERIOR plasmid, and synapsinI-positive puncta adjacent to dendrites of transfected cells were counted and compared with untransfected cells (Fig. 4 B). As expected, we observed a significant

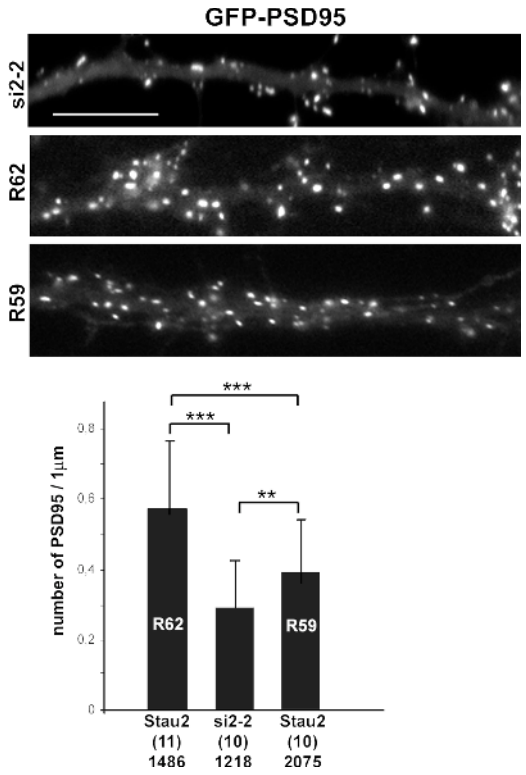


Figure 6. **Two RNAi-cleavage resistant Stau2 isoforms rescue the observed phenotype.** Representative images of dendrites of 15 DIV neurons cotransfected with the pSUPERIOR vector expressing both Stau2 shRNA and GFP-PSD95 together with the EYFP-Stau2$^{62}$ (R62) and EYFP-Stau2$^{59}$ (R59) cleavage-resistant isoforms. The total number of neurons (in parentheses) and PSD95 puncta counted are listed in the graph. **, $P < 0.005$; ***, $P < 0.0001$. Bar, 10 µm.

reduction in synapsinI puncta (26%). These results indicate that the described si-Stau2 RNA approach not only drastically reduces the number of dendritic spines, but also coincides with a reduction in presynaptic inputs. This was a first hint for a possible functional deficiency of these neurons.

To establish a more convenient and faster assay to evaluate the observed effects, we cotransfected hippocampal neurons with plasmids coding for Stau2 shRNA and GFP-PSD95 (Husseini et al., 2000; Marrs et al., 2001). In this manner, GFP-PSD95 is exclusively expressed in down-regulated neurons, allowing for a thorough quantitative analysis of dendritic spines. To verify that GFP-PSD95 puncta represent bona fide synapses, we stained transfected neurons with immunopurified anti-synapsinI antibodies, a presynaptic marker. Most PSD95 puncta were found to be in close contact with synapsinI-positive spots, indicating that GFP-PSD95 marked dendritic spines have normal presynaptic inputs (Fig. 4 C and Marrs et al., 2001). In contrast to mismatch Stau2-treated and mock-transfected neurons, the number of GFP-PSD95–positive puncta in dendritic spines was significantly reduced in Stau2 down-regulated cells (Fig. 5 A). In total, the GFP-PSD95 clusters in dendritic spines decreased by 48% (Fig. 5 A, graph). We then asked whether the remaining dendritic spines in the Stau2 down-regulated neurons still have a presynaptic input, by immunostaining Stau2 shRNA-treated neurons with anti-synapsinI antibodies. Interestingly, the majority of GFP-PSD95–positive puncta in Stau2 down-regulated cells are still in close contact with presynaptic terminals (Fig. 5 B). To further rule out the possibility of unspecific shRNA effects, we coexpressed dn2 (see Fig. 3 A) together with GFP-PSD95 in mature neurons. Dn2 reduced the amount of GFP-PSD95–positive puncta to a similar extent than Stau2 shRNA. Collectively, this suggests that Stau2 is necessary for the maintenance of dendritic spines.

Because dendritic spines in cultured hippocampal neurons are observed to form as early as 10 DIV (Papa et al., 1995; Yuste and Bonhoeffer, 2001), RNAi was performed on 8 DIV neurons to investigate whether Stau2 is also necessary for dendritic spine formation (Fig. 5 A**,** 8+3 DIV). Neurons coexpressing GFP-PSD95 and either siStau2 or mismatch Stau2 were analyzed 3 d after transfection and the GFP-PSD95 puncta were counted. The number of dendritic spines in Stau2 down-regulated neurons was significantly reduced compared with either mismatch or mock-transfected neurons (Fig. 5 A, graph; unpublished data). These data, together with the previous analysis in mature neurons, suggest an important role for Stau2 in both morphogenesis and maintenance of dendritic spines.

### The observed phenotype can be rescued by overexpression of RNAi cleavage-resistant Stau2 isoforms

We cotransfected neurons with Stau2$^{R}$ plasmids that express the following two RNAi-cleavage-resistant Stau2 protein isoforms: EYFP-Stau2$^{62}$ and EYFP-Stau2$^{59}$. To limit the number of cotransfected plasmids, PSD95 cDNA was cloned in frame with EGFP that is already present in the pSUPERIOR vector. This allows for down-regulating Stau2 and expressing GFP-PSD95 using the same construct (see Materials and methods for details). The expression of either Stau2$^{62}$ or Stau2$^{59}$ rescues the observed phenotype to a significant extent. The number of GFP-PSD95 puncta in rescued cells was thereby comparable to cells that had been transfected with the mismatch Stau2 plasmid (Fig. 6), or that had been mock transfected (see Fig. 5 A). Interestingly, the 62-kD isoform was significantly more effective than the 59-kD isoform in relieving the phenotype. It is important to note that the mere overexpression of exogenous full-length Stau2 does not cause a loss in dendritic spines as observed when overexpressing the dominant-negative dn2. Collectively, the rescue of the observed phenotype is another strong indication that our RNAi approach is Stau2 specific.

### Stau2 down-regulation alters the dendritic actin cytoskeleton

Because the actin cytoskeleton plays an important role in dendritic spine homeostasis (Fischer et al., 1998; Matus, 2005), we used Alexa546-coupled phalloidin to assess the actin cytoskeleton in Stau2 down-regulated neurons. Fig. 7 shows two phalloidin-stained neurons (red), an untransfected cell (UT), and a Stau2 shRNA-treated (T) cell. Untransfected neurons had a regular subcortical F-actin staining pattern preferentially in dendritic spines (Fig. 7, inset 2, arrowheads). In contrast, F-actin organization in the dendrite itself was severely affected in neurons lacking Stau2. These cells displayed clusters of actin in the

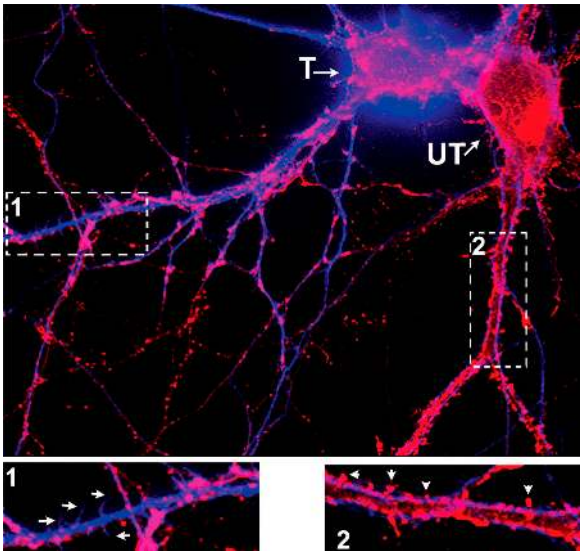


Figure 7. **Reorganization of the actin cytoskeleton in dendrites of Stau2 down-regulated neurons.** 15 DIV neurons cotransfected with si2-2 and citrine (blue) were fixed and stained for F-actin with Alexa546-labeled phalloidin (red) 3 d after transfection. In a Stau2 down-regulated cell (T), extended filopodia were detected (inset 1, arrows) and clusters of F-actin appeared in dendritic shafts. In an adjacent, untransfected cell (UT) normal, F-actin–positive dendritic spines could be observed (inset 2, arrowheads). Please note that in inset 2, axons (YFP-labeled in blue) of a Stau2 down-regulated cell still contact a dendrite of an untransfected neuron (phalloidin-labeled in red) by running on top of the dendrite.

dendrite and had extended filopodia (Fig. 7, inset 1, arrows). It is interesting to note that axons (YFP-labeled in blue) of Stau2 down-regulated cells are still able to contact a dendrite of an untransfected neuron (phalloidin-labeled in red) by running on top of the dendrite (Fig. 7, inset 2). Because the total level of actin protein in both treated and untreated neurons was not significantly altered (see Fig. S1 C), the observed differences in staining pattern are presumed to reflect a rearrangement of F-actin. The pattern of G-actin, however, was not significantly altered as assessed by DNase I-staining (unpublished data). Collectively, these results demonstrate that the actin cytoskeleton in dendrites is severely affected by the Stau2 down-regulation.

The formation of synapses is critically dependent on the actin-based motility of dendritic protrusions (Zito et al., 2004). Furthermore, β-*actin* mRNA localizes to both axonal and dendritic sites of cultured hippocampal neurons (Bassell and Singer, 1997; Tiruchinapalli et al., 2003). We, therefore, analyzed levels of β-*actin* mRNA in cell bodies as well as the number of β-*actin* mRNA-containing particles in dendrites in si2-2 and mismatch shRNA-transfected neurons by FISH. Fig. 8 A shows a Stau2 down-regulated hippocampal neuron (transfected cell expressing GFP, T) and an adjacent untransfected neuron (UT). In neuronal cell bodies, significantly lower FISH signals were detected in si2-2–transfected cells compared with untransfected cells (Fig. 8 A, see also enlarged cell bodies) and to misStau2-transfected neurons. To verify the nuclear integrity, DAPI staining was performed in transfected neurons after FISH (Fig. S2, available at http://www.jcb.org/cgi/content/full/jcb.200509035/DC1). Quantification of three independent experiments revealed a 23 ± 9% reduction of β-*actin* mRNA levels in the cell body only in si2-2–transfected neurons ($P = 0.04$, *t* test) in contrast to mismatch Stau2 transfected neurons (Fig. 8 A, top graph). Because Stau2 localizes to the dendritic compartment of neurons (Duchaîne et al., 2002), we next analyzed whether the dendritic localization of β-*actin* mRNA is changed upon Stau2 down-regulation. The enlarged insets of the indicated dendritic regions (Fig. 8 A, dendrites) of both cells clearly display a difference in the number of localized β-*actin* mRNA puncta: a reduction by 37 ± 5% compared with values obtained for mismatch Stau2-transfected neurons (Fig. 8 A, bottom graph). To demonstrate that the reduced levels of β–*actin* mRNA upon Stau2 down-regulation were not related to unspecific RNAi effects, FISH was performed to detect *GAPDH* mRNA, which is restricted to cell bodies (Fig. 8 B) and to *CaMKIIα* mRNA, which is localized to dendrites (unpublished data). In contrast to the observed effects on β-*actin* mRNA, the Stau2 down-regulation did not alter the levels nor the localization pattern of both transcripts. In conclusion, these data suggest that Stau2 down-regulation affects the levels of β-*actin* containing RNPs in polarized neurons.

### Stau2-deficient neurons display reduced mEPSC amplitudes

To reveal whether the morphological and biochemical alterations described in the previous paragraphs above are associated with functional consequences, we searched for changes in synaptic transmission. As the loss of PSD95 (Figs. 4 and 5) is suggestive of alterations in excitatory synapses, miniature excitatory postsynaptic currents (mEPSCs) through non-NMDA glutamate receptors were determined (Fig. 9). In cultures exposed to the si2-2 pSUPERIOR plasmid, the mEPSC amplitudes of transfected neurons were significantly smaller than those of nontransfected ones. In contrast, in cultures treated with the mismatch plasmid, there were no significant differences in mEPSC amplitudes between transfected and nontransfected neurons. Moreover, mEPSC amplitudes in si2-2–transfected cells were significantly smaller than those in mismatch-transfected cells. The frequencies of all the mEPSCs determined, however, were not different between si2-2–transfected and mismatch-transfected cells (0.55 Hz and 0.62 Hz, respectively; $P > 0.1$). Changes in amplitudes of mEPSCs reflect changes in postsynaptic receptor sensitivity, whereas mEPSC frequencies correspond to the probability of presynaptic vesicle exocytosis (Scanziani et al., 1992). Accordingly, the present results indicate that Stau2 down-regulation impairs excitatory synaptic transmission primarily through interference with the responsiveness of postsynaptic glutamate receptors.

## Discussion

The double-stranded RNA-binding protein Staufen plays an essential role in *Drosophila* oogenesis, early embryonic patterning, and in establishing cellular asymmetry in neuroblasts (Roegiers and Jan, 2000). Despite a plethora of information on the roles of Staufen in *Drosophila*, the functions of the mammalian homologues are still largely unknown.

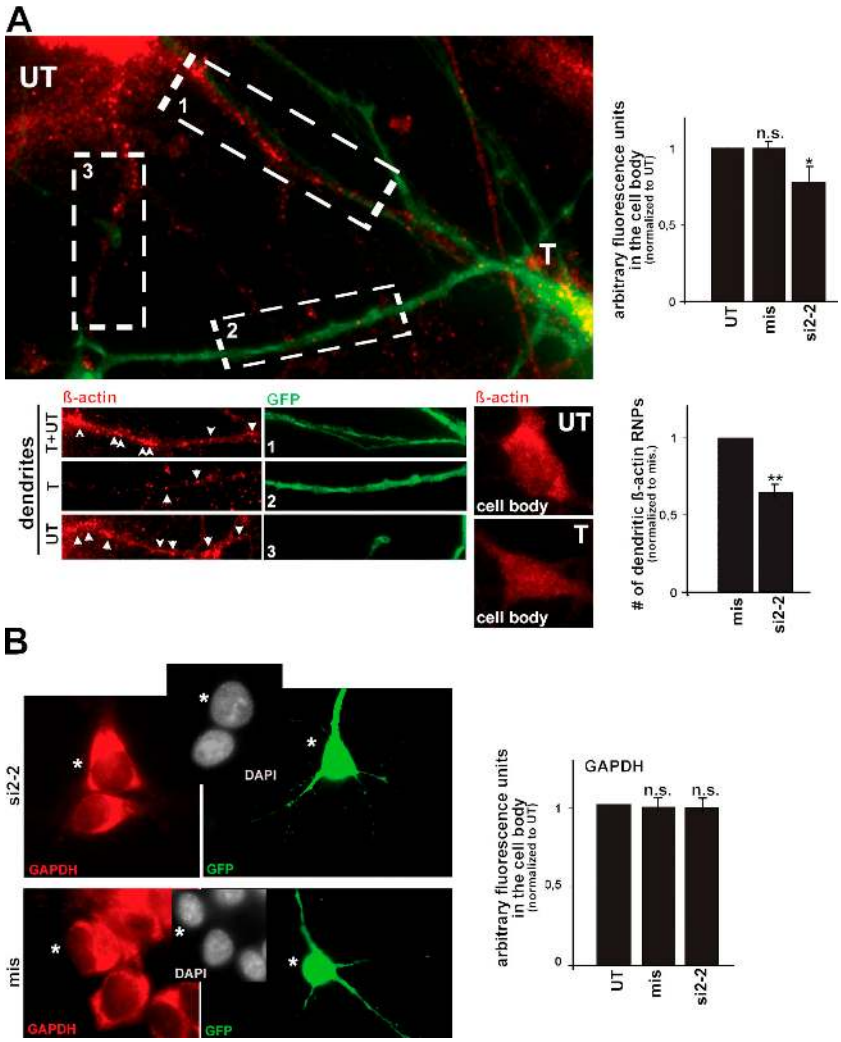


Figure 8. **Reduced β-*actin* mRNA-levels in Stau2 down-regulated neurons.** 15 DIV neurons were transfected with pSUPERIOR plasmids coding for either si2-2 or mis shRNAs. (A) FISH against β-*actin* mRNA. The number of dendritic β-*actin* particles and the somatic fluorescence intensity was determined. In Stau2 down-regulated neurons, the number of dendritic particles and the fluorescence intensity in the cell body were significantly reduced (see also insets UT and T). Arrowheads indicate dendritic β-actin RNPs. For quantification, the results from three independent experiments were averaged and values normalized to misStau2-transfected neurons (number of dendritic β-*actin* RNPs, bottom graph) or untransfected cells on the same coverslip (arbitrary fluorescence units in the cell body, top graph). $n = 15$ cells analyzed per condition. *, $P < 0.03$; **, $P < 0.005$. (B) Stau2 down-regulation does not alter *GAPDH* mRNA expression. FISH for the nonlocalized mRNA *GAPDH* was performed on neurons expressing either si2-2 or mis shRNAs. No differences in both transcription level and localization of *GAPDH* transcript were observed. The asterisk indicates the transfected neuron. $n = 15$ cells analyzed per condition. Three independent experiments were performed. Error bars represent the SD.

Stau2 is preferentially expressed in the central nervous system and here particularly in neurons (Duchaîne et al., 2002), where it is present during all stages of neuronal development and in mature neurons (Fig. S1 A and unpublished data). Previous work has implicated Stau2 in dendritic mRNA transport, which is assumed to occur solely in the cytoplasm (Roegiers and Jan, 2000; Belanger et al., 2003; Macchi et al., 2004; Miki and Yoneda, 2004; Monshausen et al., 2004). A more detailed analysis, however, provided the first evidence that both Stau1 (Martel et al., 2006) and two isoforms of Stau2, Stau2$^{62}$ and Stau2$^{59}$ (Macchi et al., 2004; Miki and Yoneda, 2004), shuttle between the nucleus and the cytoplasm using separate export pathways, suggesting distinct roles for the different Stau2 isoforms (Kiebler et al., 2005).

Aside from these indirect observations, no direct function has been assigned to any of the mammalian Staufen proteins. Because they are assumed to play a role in dendritic mRNA transport, a process generally assumed to contribute to synaptic plasticity (Steward and Schuman, 2001), we decided to investigate the function of the brain-specific Stau2 in polarized hippocampal neurons using an RNAi approach. Down-regulation of Stau2 caused (1) a loss of dendritic spines and the appearance of extended filopodia; (2) a drastic reorganization of the actin cytoskeleton in dendrites; (3) a significant reduction in β-*actin* RNA expression level in both the cell body and in dendrites of Stau2 down-regulated mature neurons; and (4) an attenuation of excitatory synaptic transmission due to a decreased postsynaptic responsiveness.

Dendritic spines are morphological specializations that protrude from the main shaft of dendrites contacting presynaptic nerve terminals (Chicurel and Harris, 1992). Although their precise function is still unclear, the generally accepted hypothesis has been put forward that "spines create a micro compartment with a range of properties that enable them to operate as a multifunctional integrative unit" (Shepherd, 1996). Dendritic spines can thereby act as semi-autonomous chemical compartments to segregate postsynaptic responses (e.g., elevated calcium) to spatially and temporarily modify molecules and to newly synthesize proteins upon synaptic activation. The formation and maintenance of dendritic spines are important for both neurogenesis and neuronal activity in the mammalian brain (Hering and Sheng, 2001; Yuste and Bonhoeffer, 2004). Considerable progress has been made toward identifying the molecules that might control dendritic spine growth and maturation

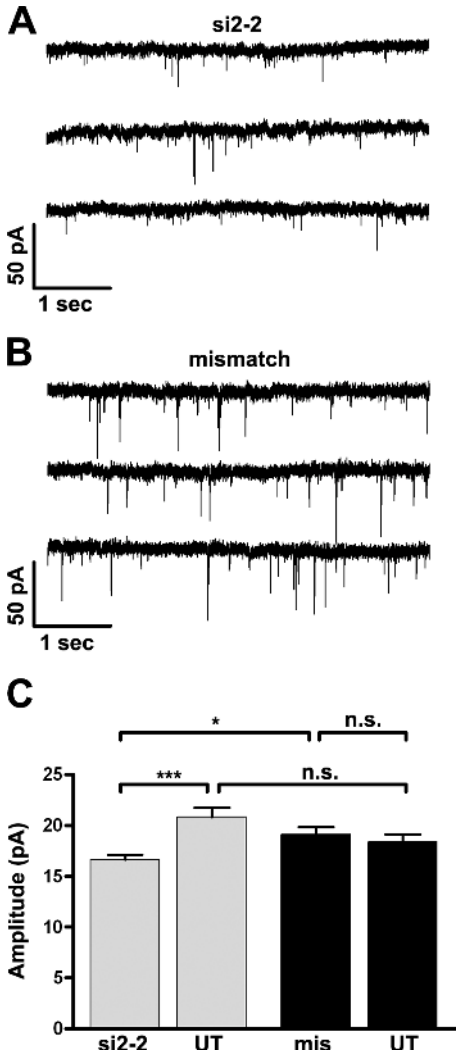


Figure 9. **Reduced mEPSC amplitudes in Stau2 down-regulated neurons.** 15 DIV hippocampal neurons were transfected with pSUPERIOR plasmids coding for either si2-2 or mis shRNAs, and mEPSCs were recorded 3 d later. (A) Original traces from one Stau2 down-regulated neuron. (B) Original traces from one mismatch-transfected neuron. (C) Comparison of mEPSC amplitudes in si2-2–transfected, mismatch-transfected, or untransfected neurons. 25 consecutive mEPSCs per neuron were recorded in 7 si2-2-transfected (si2-2) or 4 untransfected cells (UT) within 4 culture dishes exposed to si2-2 plasmids (gray bars), and in 7 mismatch-transfected (mis) or 6 untransfected neurons (UT) within 4 culture dishes treated with mismatch plasmids. ***, $P < 0.001$; *, $P < 0.05$; n.s. indicates no significant difference.

(Zhang and Benson, 2000; Hering and Sheng, 2001). Principally, the newly identified proteins fall into four categories: (1) membrane proteins (e.g., glutamate receptors, cell adhesion molecules); (2) scaffold proteins (e.g., PSD95, Shank, Homer); (3) cytoskeletal-binding/regulating proteins (e.g., actin, drebrin, spinophilin, SPAR); and (4) cytoplasmic proteins (e.g., kinases/phosphatases and other enzymes).

Recently, two other RNA-binding proteins have been implicated in dendritic spine morphogenesis, the Fragile X mental retardation protein (FMRP) and translocated in liposarcoma (TLS) (Antar and Bassell, 2003; Fujii et al., 2005). Both in Fragile X mental retardation patients (Purpura, 1974) and in adult *Fmr* knockout mice (Comery et al., 1997), unusually long and thin dendritic spines with increased density were observed. The putative functional consequences of this phenotype, e.g., on learning and memory, are currently under investigation. The increased dendritic spine density may be attributed to the absence of an activity-dependent translational repression by FMRP (Antar and Bassell, 2003). TLS, a component of heterogeneous nuclear ribonucleoprotein complexes and a nucleocytoplasmic shuttling protein, accumulates in spines at excitatory synapses upon mGluR5 activation. Hippocampal neurons derived from *tls* knockout mice, which die shortly after birth, also exhibited abnormal spine morphology: lower spine density and filopodia-like thin and long cytoplasmic protrusions (Fujii et al., 2005). A third RNA-binding protein, the zipcode binding protein 1 (ZBP1), is involved in localization of the β-*actin* message to growth cones of developing neurons and to dendrites of mature hippocampal neurons, respectively. This protein has been found to translocate from dendritic shafts into dendritic spines upon synaptic activity (Tiruchinapalli et al., 2003). Whether it is involved in dendritic spine morphogenesis, however, is unclear at present. Our studies provide first evidence that another conserved RNA-binding protein, the brain-specific Stau2, is crucial to dendritic spine formation and maintenance, suggesting that the function of RNA-binding proteins is essential to this process.

How could a defect in Stau2 cause impairment in dendritic spine morphogenesis? We have recently shown that Stau2 assembles into RNPs that move along microtubules into dendrites localizing in the proximity of the dendritic spines (Duchaîne et al., 2002; see also Fig. 2). Stau2 particles, however, do not colocalize with PSD95, a postsynaptic marker, but instead are restricted to the dendritic shaft (see Fig. 2). It is, however, possible that synaptic stimulation causes a translocation of Stau2 RNPs from the dendritic shaft to dendritic spines, as reported for TLS, FMRP, and ZBP1 (Antar and Bassell 2003; Tiruchinapalli et al., 2003; Fujii et al., 2005). This will be subject to future investigation.

It is interesting to note that the longest Stau2 isoform, Stau2$^{62}$, displays a greater ability to rescue the observed loss of dendritic spines in Stau2 down-regulated neurons. This ties in with previous findings indicating what might be distinct roles of the different Stau2 isoforms in mammalian cells. The 62-kD isoform has been shown to preferentially accumulate in the nucleolus upon down-regulation of exportin-5 (Macchi et al., 2004). Because exportin-5 has been shown to be the export factor for microRNAs from the nucleus (Yi et al., 2003; Lund et al., 2004), this suggests a possible involvement of Stau2$^{62}$ in microRNA trafficking and translational control at the synapse (Kiebler et al., 2005).

There is currently very little information on the composition of endogenous mammalian Stau2 RNPs. This is in sharp contrast to the more ubiquitously expressed Stau1 RNPs, for which both interacting proteins and putative cargo RNAs have recently been reported (Ohashi et al., 2002; Mallardo et al., 2003; Brendel et al., 2004; Kanai et al., 2004; Villace et al., 2004). To our knowledge, not a single RNA has been identified as a bona fide cargo for Stau2. Our findings that down-regulation of Stau2 results in a reorganization of the actin cytoskeleton in dendrites and also affects the levels of β-*actin* mRNA in both

the cell body and the dendrites allow us to draw two important conclusions. First, there is a yet to be identified link between Stau2 and the actin cytoskeleton. It is particularly interesting to note in this context that F-actin, consisting of β- and γ-isoforms of actin, is highly concentrated in dendritic spines and that the actin cytoskeleton (Star et al., 2002) plays an important role in activity-dependent blockage of dendritic spine motility (Matus, 2005). Second, Stau2 may bind to β-*actin* RNA, thereby influencing either its stability and/or its dendritic transport. It is tempting to speculate that the down-regulation of Stau2 may cause a reorganization of the (dendritic) actin cytoskeleton by either affecting the stability of Stau2-interacting transcripts (e.g., β-*actin*) or by controlling the translation of transcripts coding for key players in the observed actin dynamics. There are several lines of evidence that support this notion. A Stau1-specific mRNA decay pathway has recently been discovered as a means for cells to down-regulate the expression of transcripts bound by Stau1 (Kim et al., 2005). In addition, *Drosophila* Staufen functions in translational derepression of *oskar* mRNA once the mRNA has been localized to the posterior pole (Kim-Ha et al., 1991, Micklem et al., 2000). Furthermore, a recent study provided first direct evidence that Stau1 may play a similar role in mammals by facilitating translation initiation (Dugre-Brisson et al., 2005). The challenge will now be to characterize a possible molecular mechanism of how Stau2 may affect the β-*actin* mRNA stability and/or regulate local translation of β-actin.

The link between Stau2 and the actin cytoskeleton may provide the basis for the functional alterations observed after down-regulation of Stau2. On one hand, the morphology of dendritic spines clearly depends on the presence of F-actin (Matus, 2000) and actin depolymerization leads to a loss of spines (Allison et al., 1998). On the other hand, the geometry of spines is a major determinant of the responsiveness of synaptic non-NMDA glutamate receptors (Matsuzaki et al., 2001). Thus, the reduction of mEPSC amplitudes correlates well with the molecular and morphological changes of Stau2 down-regulation and thus unveils this protein as a regulator of synaptic efficacy.

## Materials and methods

**shRNAs and constructs**

Primers complementary to two distinct regions of rat Stau2 were cloned BglII and HindIII into both the pSUPER and pSUPERIOR vectors (Oligoengine; Brummelkamp et al., 2002). The sequences of the primers (Table S1, available at http://www.jcb.org/cgi/content/full/jcb.200509035/DC1) used in this study are available upon request.

pEYFP-N1 vectors (Clontech/Invitrogen) expressing cleavage-resistant forms of Stau2$^{62}$ and Stau2$^{59}$ were created by mutagenesis using the QuickChange site-directed mutagenesis kit (Stratagene) according to the manufacturer's protocol. siRFP and misStau2 shRNAs served as negative controls.

The GFP-PSD95 construct (Marrs et al., 2001) was provided by Dr. M. Dailey (University of Iowa, Iowa City, IA) with the permission of Dr. D. Bredt (University of California, San Francisco, San Francisco, CA). To avoid cotransfection of too many plasmids, PSD95 was cloned in frame with the GFP cDNA into the pSUPERIOR vector that also contains the Stau2 shRNA (si2-2). The citrine (an EYFP variant) plasmid was provided by Dr. Virginie Georget (CNRS, Monpellier, France). The photo-activatable (PA) GFP (Patterson and Lippincott-Schwartz, 2002) was provided by Dr. Jennifer Lippincott-Schwartz (National Institutes of Health, Bethesda, MD). The mutant version of Stau2 (dn2) was created as described in Tang et al. (2001).

**Semi-quantitative PCR**

RT-PCR was performed on total RNA isolated from cultured hippocampal neurons at different days in vitro (0, 3, and 23) using the RNeasy Kit (QIAGEN). The cDNAs were then amplified in the same PCR reaction and different numbers of PCR cycles were tested to ensure that amplification was not at the level of saturation.

**HeLa cells, hippocampal cultures, and transient transfections**

HeLa cells were cultivated and transfected as described in Macchi et al. (2004). Rat hippocampal neurons were cultured (Goetze et al., 2003) and transiently transfected (Goetze et al., 2004) with the plasmid expressing citrine together with pSUPER or pSUPERIOR vectors. Neurons were fixed with 4% PFA 3 d after transfection. For PSD95 experiments, 15 DIV neurons were cotransfected with vectors coding for GFP-PSD95 and si2-2, misStan2, or dn2 in the ratio of 1:5 to avoid overexpression of GFP-PSD95.

**Immunocytochemistry and fluorescence microscopy**

The following antibodies (incubation at RT for >1 h) were used: immunopurified rabbit anti-Stau1 antibodies (1 μg/ml); anti-Stau2 antibodies (1 μg/ml); monoclonal anti-PSD95 (1:1,000; Sigma-Aldrich) and polyclonal anti-synapsinI (1:1.500; Chemicon International). Cy3-coupled goat anti–mouse and anti–rabbit IgG antibodies (1:2,000) were used as secondary antibodies (Dianova). Phalloidin staining was performed as described in Goetze et al. (2004). Fluorescent images were acquired (Goetze et al., 2004) using Axiovert 200M, Axiovert 100TV, and Axiophot microscopes (all Carl Zeiss MicroImaging, Inc.) equipped with the following objectives: 40× PlanApo oil immersion, 1.2 NA, or 63× PlanApo oil immersion, 1.4 NA (both Carl Zeiss MicroImaging, Inc.) and the following CCD cameras: Olympus F-View2 (Soft Imaging System), Spec-10 LN-1300 and CoolSnap HQ (both Princeton Instruments/Roper Scientific) and the following software: MetaMorph 6.3 (Universal Imaging Corp.) or AnalySIS Five (Soft Imaging System) and assembled using Adobe Photoshop 7.0. Pictures were not modified other than adjustments of scaling, levels, brightness, and contrast.

**Data analysis**

To determine the length of dendritic spines, 15–30 EYFP-positive dendrites were randomly selected for each condition and the number and length of all protrusions was manually determined using MetaMorph 5.6. For GFP-PSD95–expressing cells, 10 cells per condition were analyzed. Only GFP-PSD95–positive puncta that reside beside the dendritic shaft were counted and expressed as puncta per μm dendrite length using Microsoft Excel. Cells expressing high levels of GFP-PSD95 were discarded. For statistical analysis, *t* test was applied using Microsoft Excel, P values <0.001 (***) were considered as highly significant. The experimenter was not aware of the experimental conditions.

To quantify β-*actin* mRNA levels, the fluorescence intensities of si2-2 and mis-transfected cell bodies were measured and normalized to the intensities of adjacent, untransfected neurons using MetaMorph 5.6. Three independent experiments with 15 cells per condition were evaluated. Dendritic particles were manually counted and the numbers per cell compared between si2-2 and mis-transfected neurons.

**Electrophysiological recordings of miniature excitatory postsynaptic currents**

mEPSCs were determined in whole-cell patch-clamp recordings at room temperature (20–24°C) on neurons at 18 DIV using an Axopatch 200B amplifier and the Pclamp 6.0 hard- and software (Axon Instruments; see Boehm and Betz, 1997). The bathing solution contained (in mM) NaCl (140), KCl (6), $CaCl_2$ (3), $MgCl_2$ (2), glucose (20), and Hepes (10), and was adjusted to pH 7.4 with NaOH. Tetrodotoxin (TTX; 0.5 μM) and bicuculline methiodide (30 μM) were added to suppress action potential propagation and miniature inhibitory postsynaptic currents, respectively. Neurons were continuously superfused using a DAD-12 (Adams and List) application system. Electrodes were pulled from borosilicate glass capillaries (Science Products) using a Flaming-Brown puller (Sutter Instruments) to yield tip resistancies of 4.5–5.5 MΩ and were filled with a solution containing (in mM) KCl (140), $CaCl_2$ (1.6), EGTA (10), Hepes (10), Mg-ATP (2), and Li-GTP (2), adjusted to pH 7.3 with KOH.

3 d after exposure to plasmids, mEPSCs were recorded from either transfected or nontransfected cells present within the same culture dish for periods of time sufficiently long to obtain at least 25 consecutive events. Thereafter, 10 μM cyano-2,3-dihydroxi-7-nitroquinoxaline (CNQX) was applied, which blocks all mEPSCs in the presence of $Mg^{2+}$ (Boehm and Betz, 1997).

mEPSCs were evaluated using the Mini Analysis Program (Synaptosoft Inc.) and detection thresholds were adjusted for each cell by analysis of traces obtained in the presence of 10 μM CNQX. mEPSCs and their inter-event intervals were tested for normal distribution by a Kolmogorov-Smirnov test and then compared by a one-way analysis of variance. The results show arithmetic means ± SEM, and P values below 0.05 were taken as indication of statistical significance.

### FISH

Endogenous β-*actin* mRNA was detected by two different approaches. First, a 500-bp RNA probe complimentary to bases 21–520 of rat β-*actin* mRNA (NM 031144) was used according to Thomas et al. (2005). After hybridization at 52°C, cells were blocked and the probes were detected using rhodamine-labeled anti-Dig Fab fragments (Roche) according to the manufacturer's instructions. Alternatively, a mix of four antisense oligonucleotides was applied (Bassell et al., 1998). These oligonucleotides were then modified with digoxigenin at the 3′-end by terminal transferase (according to the manufacturer's instructions; Roche). FISH was performed using a GAPDH antisense probe (M17701, nucleotides 4–1233) as described in Macchi et al. (2003).

### Western blotting

Neurons were transfected by nucleoporation (Amaxa) with a total of 3 μg DNA (ratio of the shRNA and citrine was 1:1) or Dharmacon oligos alone according to the manufacturer's specifications (program O-03) with the following modifications: neurons were plated directly in growth medium and petri dishes were coated with 0.1 mg/ml poly-L-lysine in borate buffer (Goetze et al. 2003).

### Online supplemental material

Fig. S1: (A) Semi-quantitative PCR performed on RNA extract from E17 hippocampal neurons at different DIV. (B) RNAi for Stau2 in HeLa cells. (C) Western blot of nucleoporated neurons. (D) Quantitative analysis of the length of all protrusions. Fig. S2: Integrity of nuclei in transfected neurons. Table S1: List of oligonucleotides used in this study. Online supplemental material available at http://www.jcb.org/cgi/content/full/jcb.200509035/DC1.

This paper is dedicated to Friedrich Bonhoeffer for his long-term support and advice. We thank Dr. E. Arn, B. Grunewald, N. Realini, A. Vaccani, and J. Vessey for assistance and Drs. R. Dahm and S. Huck for advice. Plasmids were provided by Drs. M. Dailey, D. Bredt, V. Georget, and J. Lippincott-Schwartz.

This work was supported by the SFB446, the Hertie-Stiftung, the Schram-Stiftung, the Austrian Science Fund (P17611 to S. Boehm), the Boehringer Ingelheim Foundation (to F. Tuebing), and a Human Frontier Science Program network.

Submitted: 6 September 2005
Accepted: 16 December 2005

## References

Allison, D.W., V.I. Gelfand, I. Spector, and A.M. Craig. 1998. Role of actin in anchoring postsynaptic receptors in cultured hippocampal neurons: differential attachment of NMDA versus AMPA receptors. *J. Neurosci.* 18:2423–2436.

Allison, R., K. Czaplinski, A. Git, E. Adegbenro, F. Stennard, E. Houliston, and N. Standart. 2004. Two distinct Staufen isoforms in Xenopus are vegetally localized during oogenesis. *RNA.* 10:1751–1763.

Antar, L.N., and G.J. Bassell. 2003. Sunrise at the synapse: the FMRP mRNP shaping the synaptic interface. *Neuron.* 37:555–558.

Bassell, G., and R.H. Singer. 1997. mRNA and cytoskeletal filaments. *Curr. Opin. Cell Biol.* 9:109–115.

Bassell, G.J., H. Zhang, A.L. Byrd, A.M. Femino, R.H. Singer, K.L. Taneja, L.M. Lifshitz, I.M. Herman, and K.S. Kosik. 1998. Sorting of beta-actin mRNA and protein to neurites and growth cones in culture. *J. Neurosci.* 18:251–265.

Belanger, G., M.A. Stocksley, M. Vandromme, L. Schaeffer, L. Furic, L. DesGroseillers, and B.J. Jasmin. 2003. Localization of the RNA-binding proteins Staufen1 and Staufen2 at the mammalian neuromuscular junction. *J. Neurochem.* 86:669–677.

Boehm, S., and H. Betz. 1997. Somatostatin inhibits excitatory transmission at rat hippocampal synapses via presynaptic receptors. *J. Neurosci.* 17:4066–4075.

Brendel, C., M. Rehbein, H.J. Kreienkamp, F. Buck, D. Richter, and S. Kindler. 2004. Characterization of Staufen 1 ribonucleoprotein complexes. *Biochem. J.* 384:239–246.

Broadus, J., S. Fuerstenberg, and C.Q. Doe. 1998. Staufen-dependent localization of *prospero* mRNA contributes to neuroblast daughter-cell fate. *Nature.* 391:792–795.

Brownawell, A.M., and I.G. Macara. 2002. Exportin-5, a novel karyopherin, mediates nuclear export of double-stranded RNA-binding proteins. *J. Cell Biol.* 156:53–64.

Brummelkamp, T.R., R. Bernards, and R. Agami. 2002. A system for stable expression of short interfering RNAs in mammalian cells. *Science.* 296:550–553.

Chicurel, M.E., and K.M. Harris. 1992. Three-dimensional analysis of the structure and composition of CA3 branched dendritic spines and their synaptic relationships with mossy fiber boutons in the rat hippocampus. *J. Comp. Neurol.* 325:169–182.

Comery, T.A., J.B. Harris, P.J. Willems, B.A. Oostra, S.A. Irwin, I.J. Weiler, and W.T. Greenough. 1997. Abnormal dendritic spines in fragile X knockout mice: maturation and pruning deficits. *Proc. Natl. Acad. Sci. USA.* 94:5401–5404.

Duchaîne, T.F., I. Hemraj, L. Furic, A. Deitinghoff, M.A. Kiebler, and L. DesGroseillers. 2002. Staufen2 isoforms localize to the somatodendritic domain of neurons and interact with different organelles. *J. Cell Sci.* 115:3285–3295.

Dugre-Brisson, S., G. Elvira, K. Boulay, L. Chatel-Chaix, A.J. Mouland, and L. DesGroseillers. 2005. Interaction of Staufen1 with the 5′ end of mRNA facilitates translation of these RNAs. *Nucleic Acids Res.* 33:4797–4812.

Fischer, M., S. Kaech, D. Knutti, and A. Matus. 1998. Rapid actin-based plasticity in dendritic spines. *Neuron.* 20:847–854.

Fujii, R., S. Okabe, T. Urushido, K. Inoue, A. Yoshimura, T. Tachibana, T. Nishikawa, G.G. Hicks, and T. Takumi. 2005. The RNA binding protein TLS is translocated to dendritic spines by mGluR5 activation and regulates spine morphology. *Curr. Biol.* 15:587–593.

Goetze, B., B. Grunewald, M.A. Kiebler, and P. Macchi. 2003. Coupling the iron-responsive element to GFP—an inducible system to study translation in a single living cell. *Sci. STKE.* 2003:PL12.

Goetze, B., B. Grunewald, S. Baldassa, and M.A. Kiebler. 2004. Chemically controlled formation of a DNA/calcium phosphate coprecipitate: Application for transfection of mature hippocampal neurons. *J. Neurobiol.* 60:517–525.

Hamm, A., N. Krott, I. Breibach, R. Blindt, and A.K. Bosserhoff. 2002. Efficient transfection method for primary cells. *Tissue Eng.* 8:235–245.

Hering, H., and M. Sheng. 2001. Dendritic spines: structure, dynamics and regulation. *Nat. Rev. Neurosci.* 2:880–888.

Husseini, A.E.D., E. Schnell, D.M. Chetkovich, R.A. Nicoll, and D.S. Bredt. 2000. PSD95 involvement in maturation of excitatory synapses. *Science.* 290:1364–1368.

Kanai, Y., N. Dohmae, and N. Hirokawa. 2004. Kinesin transports RNA: Isolation and characterization of an RNA-transporting granule. *Neuron.* 43:513–525.

Kiebler, M.A., and L. DesGroseillers. 2000. Molecular insights into mRNA transport and local translation in the mammalian nervous system. *Neuron.* 25:19–28.

Kiebler, M.A., I. Hemraj, P. Verkade, M. Köhrmann, P. Fortes, R.M. Marión, J. Ortín, and C.G. Dotti. 1999. The mammalian Staufen protein localizes to the somatodendritic domain of cultured hippocampal neurons: implications for its involvement in mRNA transport. *J. Neurosci.* 19:288–297.

Kiebler, M.A., R.P. Jansen, R. Dahm, and P. Macchi. 2005. A putative nuclear function for mammalian Staufen. *Trends Biochem. Sci.* 30:228–231.

Kim, I.J., H.N. Beck, P.J. Lein, and D. Higgins. 2002. Interferon gamma induces retrograde dendritic retraction and inhibits synapse formation. *J. Neurosci.* 22:4530–4539.

Kim, Y.K., L. Furic, L. Desgroseillers, and L.E. Maquat. 2005. Mammalian Staufen1 recruits Upf1 to specific mRNA 3′UTRs so as to elicit mRNA decay. *Cell.* 120:195–208.

Kim-Ha, J., J.L. Smith, and P.M. Macdonald. 1991. *oskar* mRNA is localized to the posterior pole of the *Drosophila* oocyte. *Cell.* 66:23–35.

Li, P., X. Yang, M. Wasser, Y. Cai, and W. Chia. 1997. Inscuteable and Staufen mediate asymmetric localization and segregation of *prospero* RNA during *Drosophila* neuroblast cell divisions. *Cell.* 90:437–447.

Lund, E., S. Guttinger, A. Calado, J.E. Dahlberg, and U. Kutay. 2004. Nuclear export of microRNA precursors. *Science.* 303:95–98.

Macchi, P., I Hemraj, B. Goetze, B. Grunewald, M. Mallardo, M.A. Kiebler. 2003. A GFP-based system to uncouple mRNA transport from translation in a single living neuron. *Mol. Biol. Cell.* 14:1570–1582.

Macchi, P., A.M. Brownawell, B. Grunewald, L. DesGroseillers, I.G. Macara, and M.A. Kiebler. 2004. The brain-specific double-stranded RNA-binding protein Staufen2: nucleolar accumulation and isoform-specific exportin-5-dependent export. *J. Biol. Chem.* 279:31440–31444.

Mallardo M, A. Deitinghoff, J Muller, B. Goetze, P. Macchi, C. Peters, M.A. Kiebler. 2003 Isolation and characterization of Staufen-containing ribonucleoprotein particles from rat brain. *Proc. Natl. Acad. Sci. USA*. 100:2100-2105.

Marrs, G.S., S.H. Green, and M.E. Dailey. 2001. Rapid formation and remodeling of postsynaptic densities in developing dendrites. *Nat. Neurosci.* 4:1006–1013.

Martel, C., P. Macchi, L. Furic, M.A. Kiebler, and L. Desgroseillers. 2006. Staufen1 is imported into the nucleolus via a bipartite nuclear localization signal and several modulatory determinants. *Biochem. J.* 393:245–254.

Matsuzaki, M., G.C. Ellis-Davies, T. Nemoto, Y. Miyashita, M. Iino, and H. Kasai. 2001. Dendritic spine geometry is critical for AMPA receptor expression in hippocampal CA1 pyramidal neurons. *Nat. Neurosci.* 4:1086–1092.

Matus, A. 2000. Actin-based plasticity in dendritic spines. *Science.* 290:754–758.

Matus, A. 2005. Growth of dendritic spines: a continuing story. *Curr. Opin. Neurobiol.* 15:67–72.

Micklem, D.R., J. Adams, S. Grunert, and D. St Johnston. 2000. Distinct roles of two conserved Staufen domains in oskar mRNA localization and translation. *EMBO J.* 19:1366–1377.

Miki, T., and Y. Yoneda. 2004. Alternative splicing of Staufen2 creates the nuclear export signal for CRM1 (Exportin 1). *J. Biol. Chem.* 279:47473–47479.

Monshausen, M., N.H. Gehring, and K.S. Kosik. 2004. The mammalian RNA-binding protein Staufen2 links nuclear and cytoplasmic RNA processing pathways in neurons. *Neuromolecular Med.* 6:127–144.

Ohashi, S., K. Koike, A. Omori, S. Ichinose, S. Ohara, S. Kobayashi, T.A. Sato, and K. Anzai. 2002. Identification of mRNA/protein (mRNP) complexes containing Puralpha, mStaufen, fragile X protein, and myosin Va and their association with rough endoplasmic reticulum equipped with a kinesin motor. *J. Biol. Chem.* 277:37804–37810.

Papa, M., M.C. Bundman, V. Greenberger, and M. Segal. 1995. Morphological analysis of dendritic spine development in primary cultures of hippocampal neurons. *J. Neurosci.* 15:1–11.

Patterson, G.H., and J. Lippincott-Schwartz. 2002. A photoactivatable GFP for selective photolabeling of proteins and cells. *Science.* 297:1873–1877.

Purpura, D.P. 1974. Dendritic spine "dysgenesis" and mental retardation. *Science.* 186:1126–1128.

Roegiers, F., and Y.N. Jan. 2000. Staufen: a common component of mRNA transport in oocytes and neurons? *Trends Cell Biol.* 10:220–224.

Scanziani, M., M. Capogna, B.H. Gähwiler, and S.M. Thompson. 1992. Presynaptic inhibition of miniature excitatory synaptic currents by baclofen and adenosine in the hippocampus. *Neuron.* 9:919–927.

Shepherd, G.M. 1996. The dendritic spine: a multifunctional integrative unit. *J. Neurophysiol.* 75:2197–2210.

Sledz, C.A., M. Holko, M.J. de Veer, R.H. Silverman, and B.R. Williams. 2003. Activation of the interferon system by short-interfering RNAs. *Nat. Cell Biol.* 5:834–839.

St Johnston, D. 2005. Moving messages: the intracellular localization of mRNAs. *Nat. Rev. Mol. Cell Biol.* 6:363–375.

Star, E.N., D.J. Kwiatkowski, and V.N. Murthy. 2002. Rapid turnover of actin in dendritic spines and its regulation by activity. *Nat. Neurosci.* 5:239–246.

Steward, O., and E.M. Schuman. 2001. Protein synthesis at synaptic sites on dendrites. *Annu. Rev. Neurosci.* 24:299–325.

Tang, S.J., D. Meulemans, L. Vazquez, N. Colaco, and E. Schuman. 2001. A role for a rat homolog of staufen in the transport of RNA to neuronal dendrites. *Neuron.* 32:463–475.

Thomas, M.G., L.J. Martinez Tosar, M. Loschi, J.M. Pasquini, J. Correale, S. Kindler, and G.L. Boccaccio. 2005. Staufen recruitment into stress granules does not affect early mRNA transport in oligodendrocytes. *Mol. Biol. Cell.* 16:405–420.

Tiruchinapalli, D.M., Y. Oleynikov, S. Kelic, S.M. Shenoy, A. Hartley, P.K. Stanton, R.H. Singer, and G.J. Bassell. 2003. Activity-dependent trafficking and dynamic localization of ZBP1 and β-*actin* mRNA in dendrites and spines of hippocampal neurons. *J. Neurosci.* 23:3251–3256.

Villace, P., R.M. Marion, and J. Ortin. 2004. The composition of Staufen-containing RNA granules from human cells indicates their role in the regulated transport and translation of messenger RNAs. *Nucleic Acids Res.* 32:2411–2420.

Yi, R., Y. Qin, I.G. Macara, and B.R. Cullen. 2003. Exportin-5 mediates the nuclear export of pre-microRNAs and short hairpin RNAs. *Genes Dev.* 17:3011–3016.

Yoon, Y.J., and K.L. Mowry. 2004. *Xenopus* Staufen is a component of a ribonucleoprotein complex containing *Vg1* RNA and kinesin. *Development.* 131:3035–3045.

Yuste, R., and T. Bonhoeffer. 2001. Morphological changes in dendritic spines associated with long-term synaptic plasticity. *Annu. Rev. Neurosci.* 24:1071–1089.

Yuste, R., and T. Bonhoeffer. 2004. Genesis of dendritic spines: insights from ultrastructural and imaging studies. *Nat. Rev. Neurosci.* 5:24–34.

Zhang, W., and D.L. Benson. 2000. Development and molecular organization of dendritic spines and their synapses. *Hippocampus.* 10:512–526.

Zito, K., G. Knott, G.M. Shepherd, S. Shenolikar, and K. Svoboda. 2004. Induction of spine growth and synapse formation by regulation of the spine actin cytoskeleton. *Neuron.* 44:321–334.